Decomposition Mechanism of the Anions Generated by Atmospheric Pressure Chemical Ionization of Nitroanilines

Vinh Son Nguyen,[†,‡] Chris Vinckier,[†] Tran Thanh Hue,[‡] and Minh Tho Nguyen*[,†]

Department of Chemistry, University of Leuven, Celestijnenlaan 200F, B-3001 Leuven, Belgium, and Group of Computational Chemistry, Faculty of Chemistry, University of Education, Hanoi, Vietnam

Received: June 28, 2005; In Final Form: October 4, 2005

The decomposition reaction mechanism of the anions generated by atmospheric pressure chemical ionization (APCI) mass spectrometry, in the negative mode, of nitroanilines and 2,4-dinitroanilines has been probed using quantum chemical calculations. The same process has been analyzed for the neutral counterparts and the simpler neutral and anionic nitrobenzenes. Our computations using density functional theory at the B3LYP/6-311++G(3df,2p) level demonstrate that the decomposition of the anion occurs in a two-stage process, involving an initial nitro−nitrite rearrangement followed by a NO-elimination leading to formation of a phenoxy radical anion derivative. The former is by far the rate-determining step. Calculations using the MP2 and CCSD(T)/6-311++G(d,p) levels also pointed out the same energy landscape. A similar mechanism has also been emphasized for the neutral counterparts. The effects of the amino and nitro groups as well as that of the negative charge on the nitro−nitrite interconversion are rather small and do not qualitatively modify the landscape of the pertinent energy surface and thereby the NO-loss mechanism.

1. Introduction

The terpenes chemistry plays a significant role in the global climate change context. In this field, a major challenge is the identification and quantification of the semivolatile compounds formed as their oxidation products.[1] In the same vein, mono- and diketones, aldehydes, and carboxylic acids constitute a major analytical challenge. Monitoring of carbonyl compounds in air, as used by respected environmental agencies, is based on the acid-catalyzed formation of aldehydes and ketones with 2,4-dinitrophenylhydrazine (2,4-DNPH) leading to stable 2,4-dinitrophenylhydrazone compounds.[1b,2] To analyze the chemical composition of the latter, a novel technique has recently been developed on the basis of high-performance liquid chromatography−mass spectrometry (HPLC−MS) detection in an ion trap mass spectrometer equipped with both atmospheric pressure chemical ionization (APCI) and electrospray ionization (ESI) sources.[3−5]

Compared to the widely used electron impact ionization methods, the APCI method, in its negative mode APCI(−), is a soft ionization technique causing only minor fragmentations.[6] Accordingly, a proton is abstracted from the parent molecule M leading to the formation of the parent anion $(M-H)^-$. Further information on the characteristics of the parent ion $(M-H)^-$ could be obtained from the MS/MS spectra generated by the collision-induced decomposition (CID) of this parent ion $(M-H)^-$. The ability of recording fragmentation spectra of unknown compounds allows an unambiguous determination of its structure. However, a major drawback of this technique concerns the interpretation of the fragmentation spectra of the negative ions $(M-H)^-$.

In our experimental study on the identification of the products formed in the α-pinene reactions with hydroxyl radicals, an in situ reaction occurs with the 2,4-DNPH coating layer on a liquid nitrogen trap. However, it was observed that some unwanted side reactions between the coating material and hydroxyl radicals led to the formation of 2,4-dinitroaniline.[4] This compound, which was not related to the terpene chemistry, could be identified by its fragmentation spectrum MS^2 shown in Figure 1. It was obtained in the negative APCI(−) mode of the instrument with hydroxyl ions OH^- and the cyanomethyl anion $(NC-CH_2^-)$ as deprotonation agents.

A typical fragmentation spectrum MS^2 of 2,4-dinitroaniline is shown in Figure 1. From the parent molecule 2,4-dinitroaniline, having a molar mass MM = 183, formation of the parent anion $(M-H)^-$ is clearly seen at the mass position *m*/*z* 182. Nevertheless, the major fragmentation peak of the anion $(M-H)^-$ is located at mass position *m*/*z* 152, which could be assigned to the parent ion from which a NO molecule is expulsed. A possible structure of this ion has been proposed, but the position from where NO is actually lost remains uncertain. The second highest fragmentation ion is at mass *m*/*z* 122, and this represents the parent ion from which two NO molecules are eliminated.

It has been reported that in protic solvents, such as water or methanol, a reduction process occurred in the APCI source, leading to the conversion of a nitro group into an amine with the apparent decrease of the ionic mass with 30 units.[7a] It is important to stress that in our experimental conditions, the full APCI MS spectrum of dinitroaniline solely shows the negative ion $(M-H)^-$ and that other ion fragments represent less than 2%. The ionic fragments produced in our MS^2 spectrum shown in Figure 1 were not formed in the APCI source but originated from collisions of the $(M-H)^-$ ion with helium atoms in the ion trap mass spectrometer.

It might be mentioned that expulsion of NO from various ionic aromatic nitro compounds M has also been seen with by negative chemical ionization (NCI) at a pressure of about 10^{-4} Torr[7b] or by collisionally activated decomposition (CAD) of the

* Corresponding author. Fax: 32-16-32 7992. E-mail: minh.nguyen@chem.kuleuven.be.
† University of Leuven.
‡ University of Education, Hanoi.

10.1021/jp0534986 CCC: $30.25
Published on Web 11/09/2005

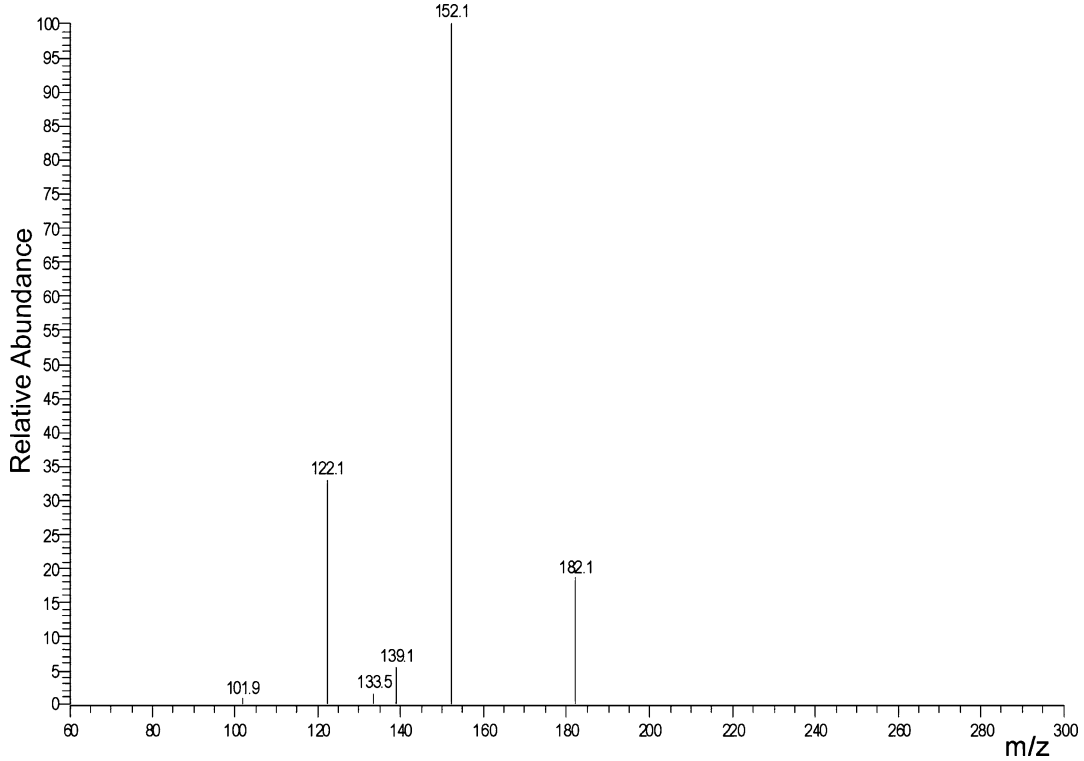

Figure 1. MS^2 fragmentation spectrum of 2,4-dinitroaniline (MM = 183). Assignment of the fragmentation ion masses is as follows: (1) m/z = 182 = $(M-H)^-$, (2) m/z = 152 = $(M-H-NO)^-$, and (3) m/z = 122 = $(M-H-NO-NO)^-$. Experimental conditions of the HPLC−MS technique (see ref 5 for details): separations were performed at 20 °C on a Hypurity C18 column from Hypersyl using a mobile phase gradient going from 50% acetonitrile/50% water up to 100% acetonitrile. The APCI vaporizer temperature was 450 °C, the discharge voltage was 6 kV, and the discharge current was 4.5 μA. The capillary temperature was 200 °C, and the capillary voltage was −4 V.

molecular anion M^-.[7c] In the latter case also an important expulsion of H_2O and an OH entity was observed.

In view of the lack of information on the mechanism of decomposition of the anions generated from the APCI(−) method, we set out to investigate the behavior of some nitroaniline derivatives, making use of quantum chemical methods, with the aim of establishing a theoretical basis for the structure of ion fragments and their fragmentation mechanism. For the purpose of comparison, and thereby comprehension, the systems investigated in this work include not only nitroanilines and dinitroanilines but also a simpler model such as nitrobenzene. For each system, in most cases, both the neutral and anionic states were examined.

2. Methods of Calculation

Standard quantum chemical calculations were carried out using both molecular orbital (MO) and density functional (DFT) theories, with the aid of the Gaussian 98[8] suite of programs. Geometrical parameters of the structures considered were initially optimized using the Hartree−Fock (HF) and DFT with the B3LYP hybrid functional[9] methods with the dp-polarization plus diffuse functions 6-311++G(d,p) basis set. The unrestricted formalism (UHF, UB3LYP) has been used for open-shell species. The character of each structure (equilibrium or transition structure) located was determined with the aid of harmonic vibrational frequencies computed at the same level. In locating the transition structures (TS), we have used the eigenvalue-following technique (EF method) implemented in Gaussian 98. Although the identity of each TS located is rather clear-cut, intrinsic reaction coordinate (IRC) calculations were carried out to verify it. Zero-point energy (ZPE) corrections to the relative energies were estimated from UB3LYP harmonic frequencies, whose values were scaled down by a factor of 0.9806. Refined geometrical parameters were subsequently optimized using the (U)B3LYP method, in conjunction with the larger 6-311++G-(3df,2p) basis set. It has been established that the B3LYP functional is a good approach for treating anions and evaluating electron affinities of radicals.[10] For the sake of comparison, in the simple model nitrobenzene system, geometry optimizations using the second-order perturbation theory (MP2) were also performed. For the latter system, single-point electronic energy calculations at the coupled-cluster theory level, CCSD(T)/6-311++G(d,p), were also carried out using both sets of geometries. Unless otherwise noted, bond distances are given in angstroms and bond angles in degrees.

3. Results and Discussion

Nitroanilines and derivatives have been the subject of extensive experimental and theoretical studies owing to their numerous applications. For example, *p*-nitroaniline is a prototype for push−pull conjugated charge-transfer molecules having large hyperpolarizability.[11] As nitroamine derivatives, nitroanilines also constitute a group of high energy density materials classified as secondary explosives.[12] It is not our purpose to examine here their various structural and molecular properties; even though they are of interest, they will not be discussed hereafter; we are rather concerned with the decomposition mechanism of their anions produced following deprotonation, implying a NO-loss. In this section, calculated results obtained for nitroanilines will first be presented, followed by those of nitrobenzenes, and finally by the 2,4-dinitroaniline system whose experimental APCI(−) mass spectrum is displayed in Figure 1. Both neutral and anionic systems will be examined.

3.1. Anions of Nitroanilines. As for a simple prototype, let us first consider the *o*-nitroaniline. Its deprotonation is possible from six distinct sites. Scheme 1 gives a summary of calculated

SCHEME 1: Calculated Relative Energies of *o*-Nitroaniline Anions at Six Distinct Deprotonation Sites[a]

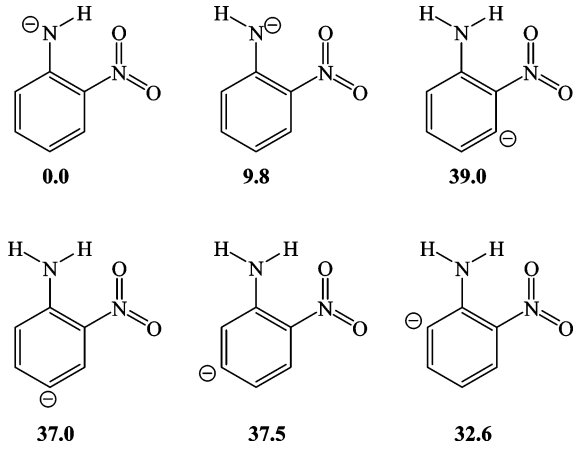

[a] Energies given in kcal/mol were obtained from B3LYP/6-311++G(3df,2p) + ZPE calculations.

relative energies of the resulting anions. It appears clear that a deprotonation from the NH bond situated in a trans position with respect to the nitro group is the most favored process. The preference of trans-NH-deprotonation by about 9 kcal/mol over the corresponding cis-NH-deprotonation is no doubt due to a stabilizing hydrogen bond-type N−H···O interaction of the resulting anion (Scheme 1). Deprotonation from CH bonds of the ring is significantly less favored, by more than 30 kcal/mol. Removal of a proton from C6 is much easier than from other C-positions; the resulting anion is somewhat stabilized by an interaction of the lone pair electron with an amine hydrogen atom.

The deprotonation energy (DPE) of *o*-nitroaniline is calculated to be DPE(N−H) = 344 kcal/mol and DPE(C−H) = 377 kcal/mol, with a probable error of ±3 kcal/mol (B3LYP/6-311++G(d,p) + ZPE). Note that for the parent aniline, the calculated value of DPE(N−H) = 366 kcal/mol[13] compares quite well with the experimental result of DPE(N−H) = 366 ± 2 kcal/mol (1533 ± 39 kJ/mol).[14] Accordingly, *o*-nitroaniline exhibits a smaller DPE than aniline and is thus a stronger acid than aniline. As a consequence, the anion is more stabilized than the neutral counterpart upon nitro substitution.

For both *m*- and *p*-nitroaniline isomers, the N−H bond remains the most favored site of deprotonation. The DPE(N−H)'s are calculated to be 348 and 340 kcal/mol in the *m*- and *p*-isomer, respectively, using the same level of theory. The latter values are comparable to the earlier experimental estimates of 352 ± 3 and 343 ± 3 kcal/mol, respectively.[15] Accordingly, the N−H acidity of nitroaniline increases in the sequence: meta < ortho < para.

For their parts, the DPE(C−H) value amounts to 374 kcal/mol at the C6-position in *m*-nitroaniline and 378 kcal/mol at the C6 (and C2)-position in *p*-nitroaniline.

Starting from the most stable N-anion of *o*-nitroaniline, a reaction pathway has been identified leading to NO-elimination. Relevant calculated results are summarized in Figures 2 and 3. Figure 2 displays a schematic potential energy profile illustrating the low-energy process yielding NO that we have found. This pathway involves two steps. The initial step is characterized by a unimolecular rearrangement converting the nitro **1** to its nitrite isomer **2**. Such a nitro−nitrite interconversion implies a transition structure **TS 1/2** for 1,2-shift around the nitro (NO_2) group in which the entire phenyl moiety is moving from N to O. The second step is an O−NO bond cleavage within the nitrite

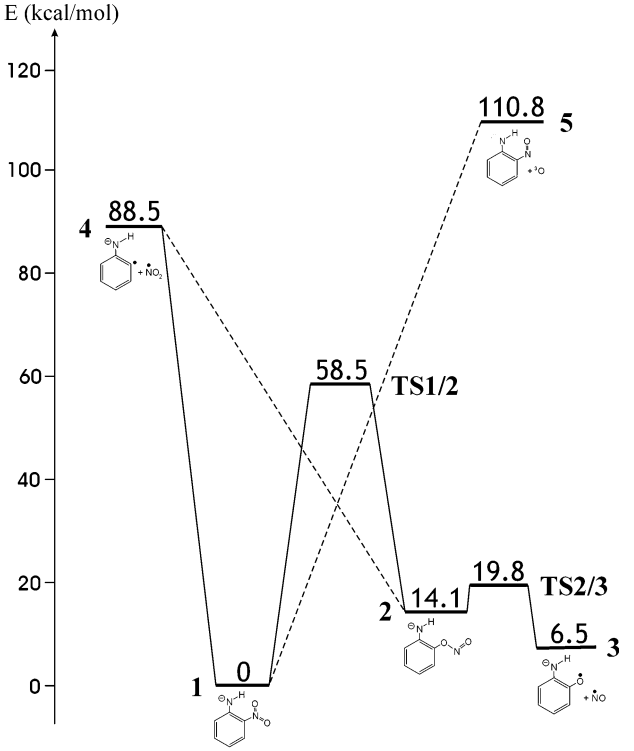

Figure 2. Schematic potential energy profile illustrating a two-stage reaction pathway in which the N-anion of *o*-nitroaniline **1** is converted to nitrite isomer **2**, followed by a NO-loss. Relative energies, given in kcal/mol, were obtained by geometry optimizations at the B3LYP/6-311++G(3df,2p) level. All values were corrected for zero-point energies evaluated using B3LYP/6-311++G(d,p) harmonic vibrational frequencies.

group producing nitric oxide NO plus the phenoxy radical anion as products **3**. The presence of the negative charge induces for this bond cleavage a transition state, which is associated with transition structure **TS 2/3**.

Selected geometrical parameters of both isomers **1** and **2** are displayed in Figure 3. The geometry and properties of **1** have been abundantly discussed in the literature and thus warrant no further comments.[16−18] Let us note that while nitroaniline **1** is planar, the nitrite isomer **2** is nonplanar in which the NO group is lying in a plane which is nearly perpendicular to the ring plane. The nitrite **2** turns out to be significantly higher in energy, up to 14 kcal/mol, than its nitro isomer **1**. The nitro−nitrite rearrangement occurred through **TS 1/2** is an energy-demanding process with a barrier height of 58 kcal/mol relative to **1**. Nevertheless, **TS 1/2** is energetically lying well below the two dissociation limits **4** and **5**, corresponding to eliminations of NO_2 and O, respectively. It is worth noting that the C−N distance of 1.53 Å in **TS 1/2** is relatively short, as compared with that of 1.96 Å previously found for the corresponding transition structure connecting the neutral nitromethane (CH_3−NO_2)−methylnitrite (CH_3−ONO) using also the B3LYP functional.[19] It has also been demonstrated that for this type of transition structure, the B3LYP, CCSD(T), and CASSCF methods provide similar results. There is no significant biradical character of the relevant TS. For the methyl pair, the energy barrier for CH_3−NO_2 to −CH_3−ONO rearrangement was calculated to be 69 kcal/mol and is slightly larger than bond dissociation energy giving CH_3 + NO_2.[19]

In contrast, the O−N bond cleavage from **2** giving the fragment products **3** via **TS 2/3** is a quite facile process, having an energy barrier of only 6 kcal/mol relative to **2**. The O−N distance of 1.95 Å in **TS 2/3** is relatively long, and the O−N

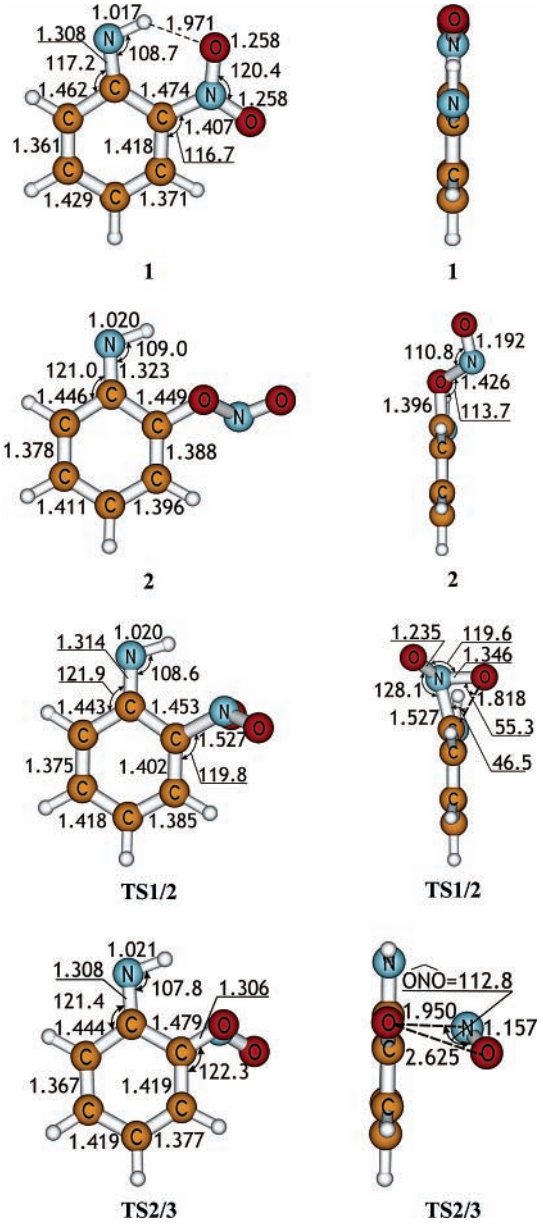

Figure 3. Selected geometrical parameters for four stationary points on the reaction pathway of the *o*-nitroaniline N-anion: nitro anion **1**, nitrite anion **2**, transition structure for nitro−nitrite rearrangement **TS1/2**, and transition structure for NO-elimination **TS2/3**. Values were obtained from B3LYP/6-311++G(3df,2p) optimizations; bond distances are given in angstroms and bond angles in degrees.

of NO points away from the ring, as indicated by the distance O−O of 2.62 Å (Figure 3). The rotation of NO around the O−N axis in **TS 2/3** is rather facile, as indicated by a shallow potential energy curve. In this context, the nitro−nitrite rearrangement **1**−**2** step constitutes the rate-determining step of the entire NO-loss process, and the nitrite isomer **2** is a quite unstable intermediate.

In view of the large O−O distance, the **TS 2/3** could exhibit a biradical character. In such a case, a multiconfigurational treatment is apparently necessary. It can be expected that a CASSCF-based treatment tends to stabilize this TS, and thereby further reduce the barrier for NO-elimination. Because the process is predominated by the **TS 1/2**, an additional stabilization of the **TS 2/3** does not induce any change in the whole process. Therefore, we did not carry out multiconfigurational computations on the **TS 2/3**.

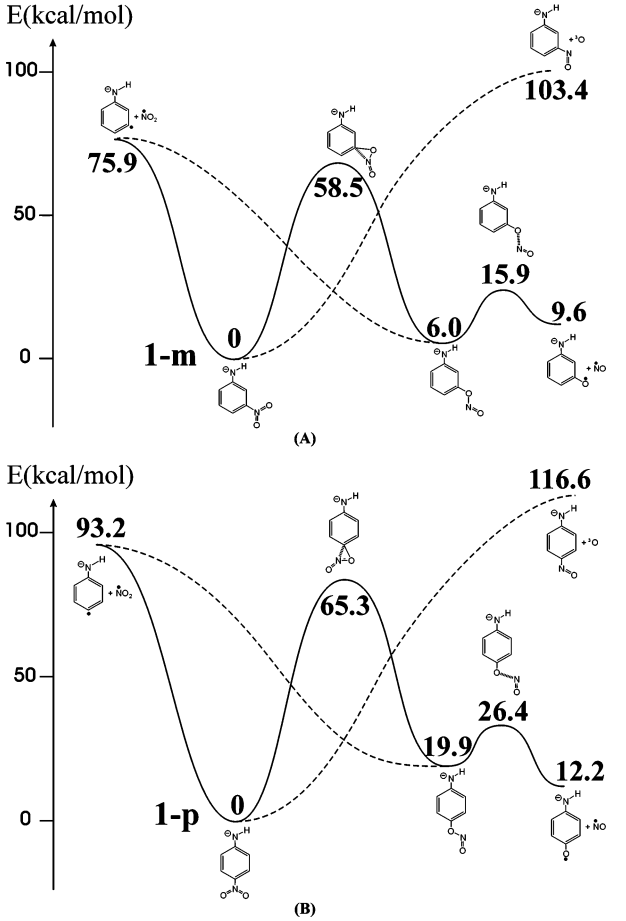

Figure 4. Two-stage reaction pathway of the N-anion of (A) *m*-nitroaniline **1-m** and (B) *p*-nitroaniline **1-p**. Relative energies, given in kcal/mol, were obtained from (U)B3LYP/6-311++G(3df,2p) + ZPE calculations.

The energy profiles illustrating the processes in both *m*- and *p*-nitroaniline N-anions are shown in Figure 4. The (U)B3LYP/6-311++G(3df,2p) + ZPE values have equally been obtained for these systems. It appears that the landscape of the potential energy surfaces remains unchanged with respect to that of the *o*-isomer, even though the relative energy positions vary here and there: (a) The nitro−nitrite energy gap varies from 14 kcal/mol in the *o*-anion to 6 kcal/mol in the *m*-anion and 20 kcal/mol in the *p*-anion. (b) The energy barrier for the 1,2-shift via **TS 1/2** is 58.5 kcal/mol for both ortho and meta, but modified to 65.3 kcal/mol for para. (c) The energy barrier for NO-loss through **TS 2/3** is also marginally changed by 1−2 kcal/mol. The relative positions are the results of different electronic factors, but it is apparently not simple to figure them out.

Overall, the NO-elimination from the N-anion of nitroaniline is likely to occur through a two-stage mechanism in which the initial nitro−nitrite rearrangement behaves as the rate-determining step, irrespective of the relative position of both groups on the benzene ring. The nitrite isomer is only a short-lived transient intermediate.

3.2. Neutral Nitroanilines. To better understand the role of the negative charge, we have investigated the NO-losses in three corresponding neutral isomers. Figure 5 displays schematic energy profiles of relevant processes in the neutral *o*-, *m*- and *p*-nitroanilines. Compared with the results for anions discussed above, a few points of interest can be noted: (i) The energy gap between both the nitro **1-N** and nitrite **2-N** isomers is substantially reduced, to 1−4 kcal/mol, even though the nitro isomer remains the more stable isomer. (ii) In the meantime,

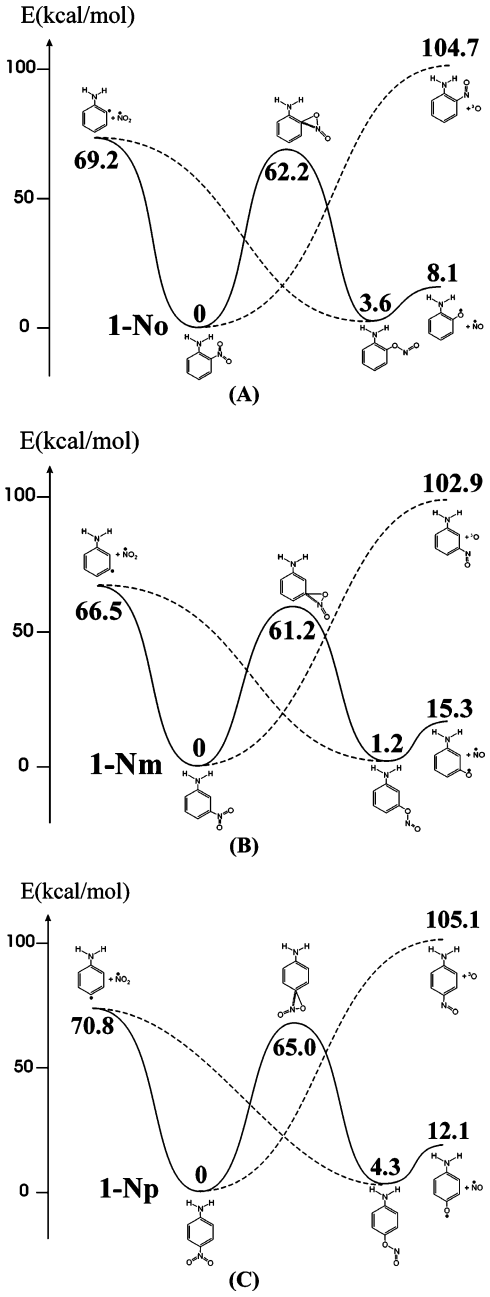

Figure 5. NO-elimination processes in neutral systems: (A) *o*-nitroaniline **1-No**, (B) *m*-nitroaniline **1-Nm**, and (C) *p*-nitroaniline **1-Np**. Relative energies, given in kcal/mol, were obtained from (U)B3LYP/6-311++G(3df,2p) + ZPE calculations.

the energy barrier for nitro−nitrite interconversion via **TS 1/2-N** is found to be increased by 4−5 kcal/mol. (iii) As a consequence, the energy separation between **TS 1/2** and the dissociation limit **4-N** arising from C−NO_2 bond cleavage is now reduced to 5−7 kcal/mol. Such a gap seems however large enough to induce a preferential rearrangement over bond cleavage. (iv) Due to the neutral character of the system, the NO-loss from **2-N** is a simple O−N bond cleavage without a transition state. Thus, the resulting dissociation limit **3-N** is lying consistently, but marginally by 4−15 kcal/mol, above the nitrite **2-N**, indicating again the low stability of the latter isomer. (v) In the **TS 1/2-N**, both the C−N and C−O distances are of comparable magnitude, and the C−N distance of 1.88 Å is markedly longer than that of 1.53 Å in the anionic system (cf. Figure 3) but approaching that of 1.96 Å in the CH_3NO_2 −CH_3-ONO rearrangement (cf. above).[19] (vi) The NO-elimination from

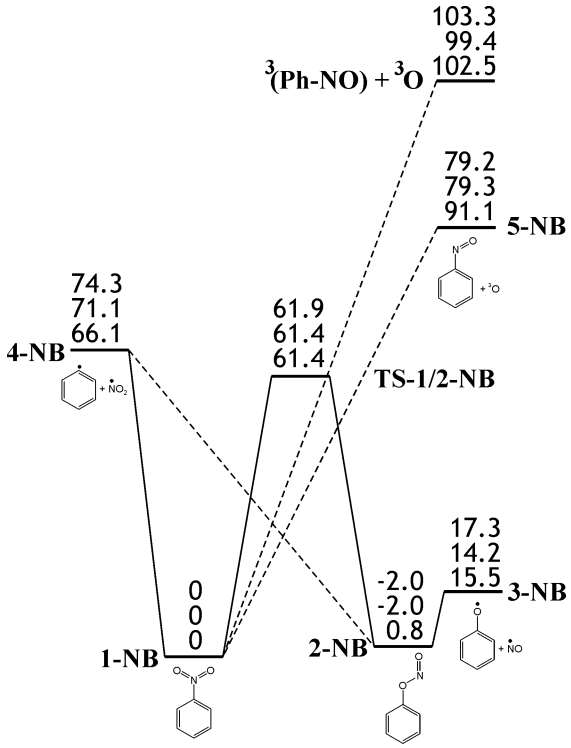

Figure 6. Reaction pathway in neutral nitrobenzene **1-NB**. Relative energies, given in kcal/mol, were obtained from the following: upper, (U)CCSD(T)/6-311++G(d,p)//(U)B3LYP/6-311++G(3df,2p); middle, (U)CCSD(T)/6-311++G(d,p)//(U)MP2/6-311++G(d,p); lower, (U)-B3LYP/6-311++G(3df,2p)//(U)B3LYP/6-311++G(3df,2p). ZPEs were from (U)B3LYP/6-311++G(d,p) vibrational frequencies.

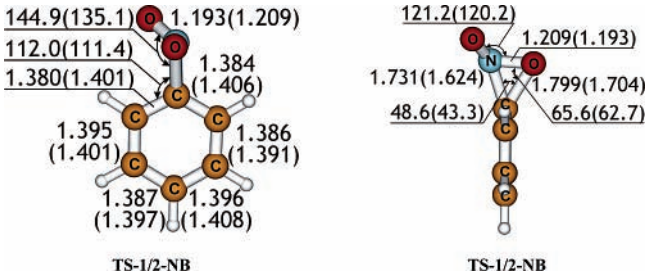

Figure 7. Selected geometrical parameters of the transition structure for nitrobenzene−phenylnitrite rearrangement **TS-1/2-NB**. Values were obtained from B3LYP/6-311++G(3df,2p) (upper values) and MP2/6-311++G(d,p) (lower values) geometry optimizations Bond distances are given in angstroms and bond angles in degrees.

neutral nitroanilines is mechanistically similar to that of their N-anions, involving a rate-determining nitro−nitrite rearrangement. The latter is actually favored by the presence of the excess electron, which induces a destabilization of the nitrite isomer, a stabilization of the fragment products, and an overall acceleration of the NO-elimination process. Nevertheless, this does not have much influence on the reaction course.

3.3. Neutral and Anionic Nitrobenzenes. To probe further the mechanistic aspect concerning the role of the amino group in the NO-loss, we have simply removed it from the system. Thus we have considered neutral nitrobenzene and its anions formed by CH-ring deprotonations. As for an attempt to calibrate the DFT results, geometry optimizations were, for this system, carried out using the second-order perturbation theory (MP2) with the 6-311++G(d,p) basis sets. Single-point electronic computations were subsequently computed at the coupled-cluster theory CCSD(T) again with the 6-311++G(d,p) basis set using both B3LYP and MP2 sets of optimized geometries. Let us

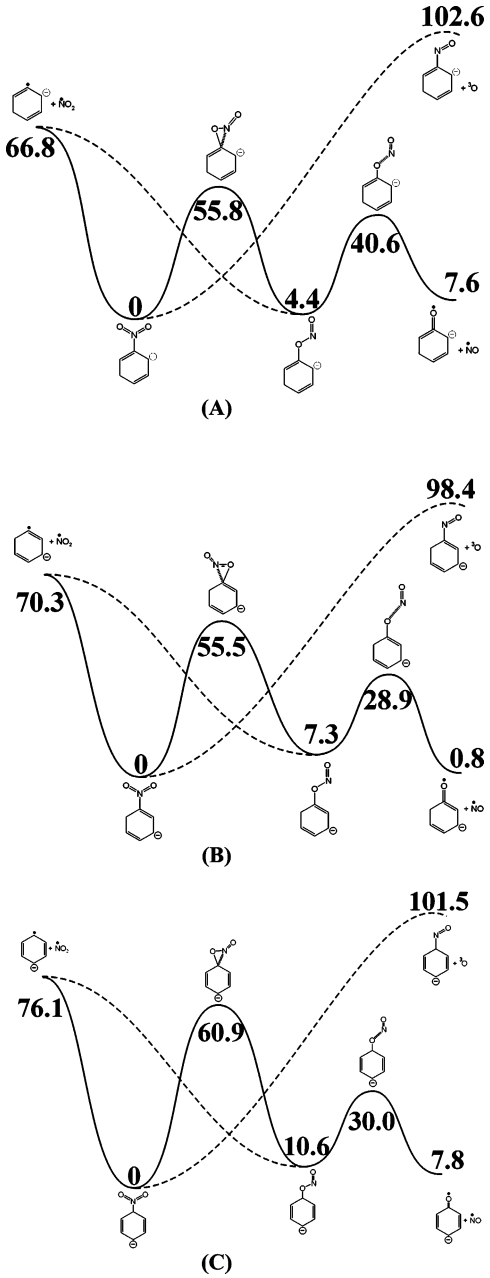

Figure 8. NO-elimination processes in anions derived from nitrobenzene: (A) *o*-anion, (B) *m*-anion, and (C) *p*-anion. Relative energies, given in kcal/mol, were obtained from (U)B3LYP/6-311++G(3df,2p) + ZPE calculations.

examine in some detail the results obtained for neutral nitrobenzene summarized in Figures 6 and 7.

For geometrical parameters of the transition structure (Figure 7), the values obtained by two distinct methods are comparable, lying within the expected differences. It is remarkable that the B3LYP relative energies are quite close to those derived from coupled-cluster CCSD(T) calculations for the positions of the minima **1-NB**, **2-NB**, and **TS 1/2-NB** (Figure 6). Compared with neutral nitroanilines described above, the energy gap in the nitrobenzene (NB, Ph−NO_2)−phenylnitrite (Ph−ONO) pair amounts to only 1 kcal/mol in favor of the nitro form at the B3LYP level; the nitrite form even becomes slightly more stable, by 2 kcal/mol, than the nitro counterpart. In addition, the nitrite isomer becomes slightly more resistant to the O−N bond cleavage. Nevertheless, the process starting from nitrobenzene remains controlled by the initial nitro−nitrite rearrangement,[19] which is characterized by transition structure **TS-1/2-NB**

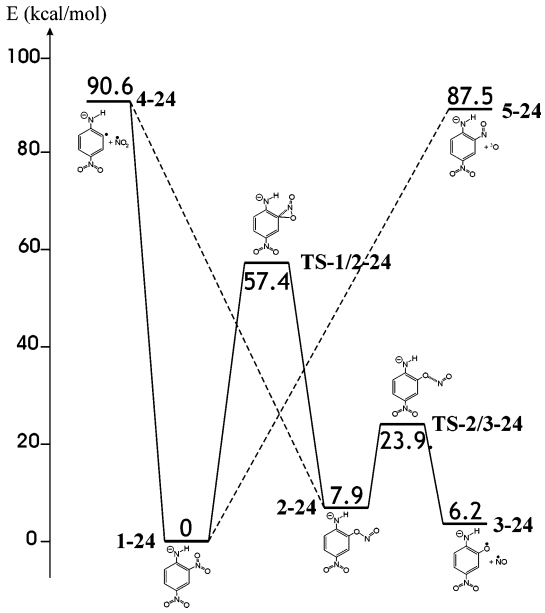

Figure 9. Schematic potential energy profile showing the processes in a N-anion of 2,4-dinitroaniline **1**−**24**. Relative energies, given in kcal/mol, were obtained from (U)B3LYP/6-311++G(3df,2p) + ZPE calculations.

depicted in Figure 7. The two characteristic parameters of the latter structure, namely the C−N and C−O distances, amount to 1.731 and 1.799 Å, respectively. These are quite close to the corresponding values of 1.655 and 1.796 Å, in neutral *o*-nitroanilines determined using the same level of theory (B3LYP/6-311++G(3df,2p)+ZPE). In addition, the energy barrier of 61.4 kcal/mol calculated for the 1,2-shift of phenyl through **TS-1/2-NB**, relative to nitrobenzene (Figure 6), is marginally smaller than that of 62.2 kcal/mol reported above for *o*-nitroaniline (Figure 5). This indicates that although the amino NH_2 group in nitroanilines exerts a small but real destabilization of the nitrite intermediate, and somehow favors the fragment products, the overall rate for NO-elimination is not significantly affected, as compared with nitrobenzene.

Additional information on the effect exerted by the negative charge on the process can be obtained from the anions formed upon C−H deprotonation of nitrobenzene. These anions are referred to as *o*-, *m*-, and *p*-NB anions, depending on the position of the position of the carbanion on the ring with respect to the NO_2 group. Note that the relevant deprotonation energies are calculated to be DPE(C−H) = 380, 382, and 381 kcal/mol, for ortho, meta, and para CH, respectively (B3LYP/-311++G(3df,2p)+ZPE values). These differ slightly from the values obtained above for nitroanilines, by a reduction of about 3 kcal/mol.

The calculated energy profiles collected in Figure 8 point out once more that a similar mechanism for NO-elimination persists in *p*-, *m*-, and *o*-nitrobenzene anions, even though thanks to the presence of the negative charge, the energy barriers for the rate-controlling nitro−nitrite interconversion step are somewhat decreased (by about 5 kcal/mol), and the barrier heights for NO-departure are increased. It should be stressed that the purpose of the present work is not a detailed study of the decomposition of nitrobenzene. We note however that involvement of phenylnitrite has been put forward to interpret the mass spectrum of nitrobenzene occurred in the radical cation state.[20]

3.4. N-Anion of 2,4-Dinitroaniline. Let us now examine a real system, which corresponds to the one utilized in the APCI

MS experiments described in Figure 1. The corresponding potential energy profile for the **1**−**24** anion is presented in Figure 9. Relative to the results derived for the *o*-nitraniline N-anion **1** discussed in section 3.1., the extra NO_2 group at the para (C4) position induces the following modifications: (i) a stabilization of 6 kcal/mol for the nitrite form by reducing the nitro−nitrite energy gap to 8 kcal/mol; (ii) a reduction of 1.1 kcal/mol on the barrier height for nitro−nitrite rearrangement which now amounts to 57.4 kcal/mol; thus the process is slightly accelerated upon second nitro substitution; (iii) there is a stabilization of 0.3 kcal/mol for the fragment products (cf. Figures 2 and 9) and in the meantime a decrease of 4 kcal/mol for the barrier for NO-elimination. Accordingly, apart from the small and rather expected changes in absolute values for relative energies between stationary points due to the presence of the second nitro group, the shape of the energy surface remains unchanged. In other words, the decomposition mechanism of this real anion is consistent with that emphasized above for simpler model systems.

Finally it should be mentioned that the energy barrier of 57.4 kcal/mol of **TS 1/2**−**24** is quite accessible by the collision-induced dissociation (CID) method in which the available energy is about 3 eV.

It would be interesting to perform similar ab initio calculations on the molecular anions M^- to check the energy barriers for the expulsion of H_2O, NO, and OH from *o*-nitrotoluene, *o*-nitrophenol, and *o*-nitroaniline in order to figure out their fragmentation pattern.[7c]

4. Concluding Remarks

In summary, we have analyzed the decomposition reaction mechanism of the anions generated by atmospheric pressure chemical ionization mass spectrometry of nitroanilines and congeners. Our quantum chemical computations demonstrate that the decomposition occurs in a two-stage process, involving an initial nitro−nitrite rearrangement followed by a NO-elimination leading to formation of a phenoxy radical anion derivative. The former is by far the rate-determining step. The effects of the amino and nitro groups attached on the ring, as well as that of the negative charge, on the nitro−nitrite interconversion are rather small and do not qualitatively modify the landscape of the pertinent potential energy surface. Anionic and neutral derivatives of nitrobenzene appear to follow the same decomposition mechanism.

Acknowledgment. We are indebted to the K.U. Leuven Research Council (GOA program). V.S.N. is grateful to the Belgian Technology Cooperation (BTC) administration for a doctoral scholarship. The Hanoi group thanks the University of Education and Vietnam Science Council (Project 561604) for support.

References and Notes

(1) (a) Brasseur, G. P.; Prin, Rg.; Pszenny, A. A. P. *Atmospheric Chemistry in a Changing World*; Springer-Verlag: Berlin, Germany, 2003; p 160. (b) Purdue, L. H.; Dayton, D. P.; Rice, J.; Busey, J. *Technical Assistance Document for Sampling and Analysis of Ozone Precursors*; EPA-600/8-91-215; U.S. Environmental Protection Agency: Research Triangle Park, NC, 1991.

(2) EMEP CCC. *Manual for Sampling and Chemical Analysis*; Report 1/95; Norwegian Institute for Air Research: Kjeller, Norway, 1996

(3) Van den Bergh, V.; Coeckelberghs, H.; Vanhees, I.; DeBoer, R. Compernolle, F.; Vinckier, C. *Anal. Bioanal. Chem.* **2002**, *372*, 630.

(4) Vanhees, I.; Van den Bergh, V.; Schildermans, R.; De Boer, R.; Compernolle, F.; Vinckier, C. *J. Chromatogr., A* **2001**, *915*, 75.

(5) Van den Bergh, V.; Coeckelberghs, H.; Vankerckhoven, H.; Compernolle, F.; Vinckier, C. *Anal. Bioanal. Chem.* **2004**, *379*, 484.

(6) De Hoffmann, E.; Charette, J.; Stroobant, V. *Mass Spectrometry, Principles and Applications*; Wiley: New York, 2003.

(7) (a) Karancsi, T.; Slegel, P. *J. Mass Spectrom.* **1999**, *34*, 975. (b) Pramanik, B. N.; Das, P. R. *Org. Mass Spectrom.* **1987**, *22*, 742. (c) McLuckey, S. A.; Glish, G. L. *Org. Mass Spectrom.* **1987**, *22*, 224.

(8) Frisch, M. J.; Trucks, G. W.; Schlegel, H. B.; Scuseria, G. E.; Robb, M. A.; Cheeseman, J. R.; Zakrzewski, V. G.; Montgomery, J. A., Jr.; Stratmann, R. E.; Burant, J. C.; Dapprich, S.; Millam, J. M.; Daniels, A. D.; Kudin, K. N.; Strain, M. C.; Farkas, O.; Tomasi, J.; Barone, V.; Cossi, M.; Cammi, R.; Mennucci, B.; Pomelli, C.; Adamo, C.; Clifford, S.; Ochterski, J.; Petersson, G. A.; Ayala, P. Y.; Cui, Q.; Morokuma, K.; Malick, D. K.; Rabuck, A. D.; Raghavachari, K.; Foresman, J. B.; Cioslowski, J.; Ortiz, J. V.; Baboul, A. G.; Stefanov, B. B.; Liu, G.; Liashenko, A.; Piskorz, P.; Komaromi, I.; Gomperts, R.; Martin, R. L.; Fox, D. J.; Keith, T.; Al-Laham, M. A.; Peng, C. Y.; Nanayakkara, A.; Gonzalez, C.; Challacombe, M.; Gill, P. M. W.; Johnson, B.; Chen, W.; Wong, M. W.; Andres, J. L.; Gonzalez, C.; Head-Gordon, M.; Replogle, E.S.; Pople, J. A. *Gaussian 98*, revision A.7; Gaussian, Inc.: Pittsburgh, PA, 1998.

(9) Parr, R. G.; Yang, W. *Density Functional Theory of Atoms and Molecules*; Oxford University Press: New York, 1989.

(10) Rienstra-Kiracofe, J. C.; Tschumper, G. S.; Schaefer, H. F.; Nandi, S.; Ellison, G. B. *Chem. Rev.* **2002**, *102*, 231.

(11) Zyss, J., Kelley, P.; Liao, P. *Molecular Nonlinear Optics: Materials, Physics and Devices*; Academic Press: Boston, 1994.

(12) Kohler, J.; Meyer, R. *Explosives*; VCH: New York, 1993.

(13) Nam, P. C.; Nguyen, M. T. Unpublished work, 2005.

(14) Bartmess, J. E.; Scott, J. A.; McIver, R. T., Jr. *J. Am. Chem. Soc.* **1979**, *101*, 6046.

(15) Taft, R. W.; Topsom, R. D. *Prog. Phys. Org. Chem.* **1987**, *16*, 1.

(16) Chen, P. C.; Chen, S. C. *Int. J. Quantum Chem.* **2001**, *83*, 332.

(17) Chen, P. C.; Chieh, Y. C.; Tzeng, S. C. *J. Mol. Struct. (THEOCHEM)* **2003**, *634*, 215.

(18) Nguyen, M. T. In *The Chemistry of Anilines*; Rappoport, Z., Ed.; Wiley: Chapter 1, to be published.

(19) Nguyen, M. T.; Le, H. T.; Hajgató, B.; Veszprémi, T.; Lin, M. C. *J. Phys. Chem. A* **2003**, *107*, 4286.

(20) Kosmidis, C.; Ledingham, K. W. D.; Kilic, H. S.; McCanny, T.; Singhal, R. P.; Langley, A. J.; Shaikh, W. *J. Phys. Chem. A* **1997**, *101*, 2264.